CrossMark

ORIGINAL RESEARCH ARTICLE

Preparation, Characterization, and Antimicrobial Properties of Chitosan–Silver Nanocomposites Films Against Fish Pathogenic Bacteria and Fungi

S. H. S. Dananjaya[1] · D. C. M. Kulatunga[1] · G. I. Godahewa[2] · Chamilani Nikapitiya[2,3] · Chulhong Oh[4] · Madurani Edussuriya[5] · Jehee Lee[2,3] · Mahanama De Zoysa[1,3]

Abstract Development of nanostructured films using natural polymers and metals has become a considerable interest in various biomedical applications. Objective of the present study was to develop silver nano particles (AgNPs) embedded chitosan films with antimicrobial properties. Based on the Ag content, two types of chitosan silver nano films, named as CAgNfs-12 (12 mM) and CAgNfs-52 (52 mM) were prepared and characterized. Field emission scanning electron microscope (FE-SEM) images of two CAgNfs showed the circular AgNPs, which were uniformly embedded and distributed in the matrix of chitosan films. Antimicrobial experiment results clearly indicated that CAgNfs can inhibit the growth of fish pathogenic bacteria *Vibrio* (*Allivibrio*) *salmonicida, V. tapetis, Edwardsiella tarda* and fungi *Fusarium oxysporum*. Moreover, CAgNfs significantly reduced the experimentally exposed *V. salmonicida* levels in artificial seawater, suggesting that these CAgNfs could be used to develop antimicrobial filters/membranes for water purifying units to eliminate the pathogenic microbes.

Graphical Abstract
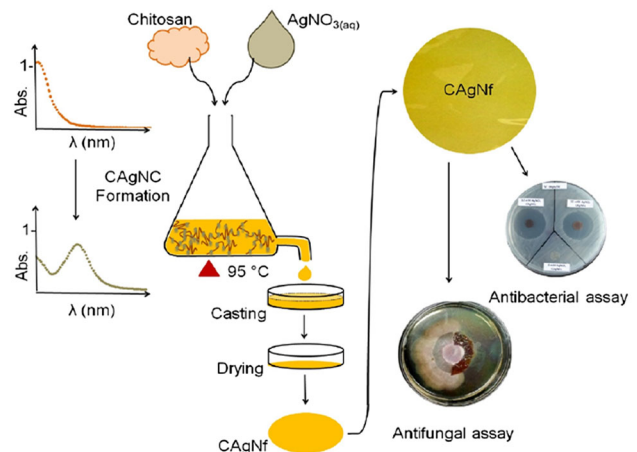
✉ Jehee Lee
jehee@jejunu.ac.kr

✉ Mahanama De Zoysa
mahanama@cnu.ac.kr

1 College of Veterinary Medicine and Research Institute of Veterinary Medicine, Chungnam National University, Daejeon 34134, Republic of Korea

2 Department of Marine Life Sciences, School of Marine Biomedical Sciences, Jeju National University, Jeju City, Jeju Self-Governing Province 63243, Republic of Korea

3 Fish Vaccine Research Center, Jeju National University, Jeju City, Jeju Self-Governing Province 63243, Republic of Korea

4 Jeju International Marine Science Research and Education Center, Korea Institute of Ocean Science and Technology, Jeju City, Jeju Self-Governing Province 63349, Republic of Korea

5 Department of Chemistry, Faculty of Science, University of Ruhuna, Matara, Sri Lanka

Introduction

Development of nanostructured films with combination of natural polymers and metals has become an important research field of nanotechnology. Nano films can be applied in various aspects in aquaculture such as in water

treatments and filtration, diseases control (as antimicrobial materials), reduce heavy metal toxicity, antifouling in aquaculture nets, and biodegradable packaging materials for seafood products [1]. The use of biopolymers for developing nano films has been increased over the past years due to their low cost, renewability, nontoxic properties and environment friendly processing methods. Among various biopolymers, polysaccharides such as starch, alginate and chitosan have been proven to be good materials [2–5].

Chitosan is a natural poly cationic linear polysaccharide composed of randomly distributed beta-(1,4)-linked D-glucosamine (deacetylated unit) and N-acetyl-D-glucosamine (acetylated unit). In general, chitosan can be produced by deacetylation of chitin, which is a structural element in crustacean exoskeleton, insect cuticle and fungal cell wall. Chitosan has been widely used for developing nano materials due to excellent properties such as biodegradability and biocompatibility [2]. Besides that, chitosan has shown a wide array of antimicrobial activities and filmogenic properties. On the other hand, nano scale silver (Ag) or silver nano particles (AgNPs) have shown strong therapeutic power, hence, those materials have been applied extensively on various biomedical applications including antimicrobial and wound dressings [6, 7]. Moreover, the use of chitosan polymers as templates and reducing agents is considered as one of the effective alternatives to synthesize AgNPs [8]. Previous reports have dealt with biopolymers like chitosan [9], heparin [10] and soluble starch [11] as reducing and stabilizing agents for preparation of AgNPs. Anastas and Williamson [12] have emphasized that nano products should be developed by green synthesis methods to reduce the formation of hazardous waste.

At present, there is a great interest to generate antibacterial films due to their superior biomedical relevance [13]. Although, many synthetic polymer based nanocomposites have been employed as surgical and wound dressings, they often generate skin irritations due to leaching of harmful chemicals, which cause numerous side effects [14]. Therefore, production of antimicrobial films using renewable natural sources like chitosan would be a better option. Recently, Rujitanaroj et al. [15] reported the antimicrobial activity of AgNPs incorporated gelatin fiber mats against *Escherichia coli, Pseudomonas aeroginosa, Staphylococcus aureus* and methicillin-resistant *S. aureus* (MRSA). To date, only few reports have been published on the development of CAgNfs which display antibacterial activities against fish pathogenic bacteria. Moreover, there are no reports on antifungal activities of CAgNfs against pathogenic *F. oxysporum*.

In this study, two types of CAgNfs (CAgNf-12 and CAgNf-52) were prepared based on the amount of Ag content by applying low molecular weight chitosan under "green synthesis approach". In order to confirm the formation of AgNPs in chitosan films, UV–Vis absorption spectrum, field emission transmission electron microscopy (FE-TEM), FE-SEM, film thickness and concentration of AgNPs in films were determined, and compared with normal chitosan film (Cf). Antimicrobial activity of CAgNfs was tested (in vitro) against fish pathogenic bacteria (*V. salmonicida, V. tapetis* and *E. tarda)* and fungi *F. oxysporum*. Our results showed that CAgNfs can inhibit the growth of bacteria (*V. salmonicida, V. tapetis* and *E. tarda*) and fungi (*F. oxysporum*). To the best of our knowledge, this is the first report related to the antimicrobial activity of CAgNfs against fish pathogenic bacteria and fungi.

Materials and Methods

Materials

Low molecular weight chitosan, silver nitrate ($AgNO_3$), nitric acid (HNO_3), acetic acid (CH_3COOH) and sodium hydroxide (NaOH) were purchased from Sigma Aldrich (USA). Marine broth (MB), potato dextrose broth (PDB), marine agar (MA) and potato dextrose agar (PDA) were purchased from Becton, Dickinson (USA). Carbon film on 300 mesh copper grids (CF300-CU) were purchased from Electron Microscopy Sciences (USA).

Preparation of CAgNfs

CAgNf-12 and CAgNf-52 were prepared based on the amount of Ag content. Chitosan stock solutions were prepared as described by Regiel et al. [16]. Briefly, chitosan solution (1% w/v) was prepared using acetic acid (0.5 M) by heating the mixture at 65 °C under continuous stirring till it becomes a homogenous solution. This chitosan solution (50 mL) was further heated up to 95 °C while stirring, and 20 mL of 12 mM $AgNO_3$ solution was added dropwise under heating to prepare CAgNf-12. Similar procedure was followed for the preparation of CAgNf-52 using 52 mM $AgNO_3$ solution. The dispersions were kept under stirring for 3 h, and formation of colloidal chitosan silver nanocomposites (CAgNCs) were confirmed by gradual darkening of the solution. Films were produced by drying the CAgNCs solution according to the solvent evaporation method. Briefly, colloidal CAgNCs (25 mL) were poured into the petri dishes (internal diameter −9 cm) and dried at 50 °C to evaporate acetic acid. The final product of CAgNfs was neutralized with 4% (w/v) NaOH, and then washed with deionized water. The CAgNfs were dried in the furnace at 60 °C, and stored in the dark until further use.

Physicochemical Characterization of CAgNfs

To determine the formation of AgNPs in film matrix, UV–Vis absorption spectrum of colloidal CAgNCs solution was recorded over a wavelength range from 300 to 500 nm using a spectrophotometer (Mecasys, Republic of Korea). The size and morphology of AgNPs in CAgNCs solution were determined by TEM (Model Tecnai G2 F30 S-Twin, FEI, USA). Briefly, few drops of CAgNCs solution were placed on carbon coated copper grid, and subsequently dried in air before transferring into the electron microscope which was operated at an accelerating voltage of 300 kV. Particle size and zeta potential were determined at 25 °C using Zetasizer S-90 Malvern instruments (Malvern, UK). The thickness of the CAgNfs was measured in 10 different regions using a digital thickness gauge (Baxlo Micrometer 3006, Spain). Water uptake test was carried out according to the method described by Sharma et al. [4]. Briefly, triplicate samples of each film were weighed using a weighing balance (HR-250 AZ, Japan) and equilibrated in 10 mL of phosphate buffered saline (PBS) (pH 7.4) at room temperature. After 24 h, the films were taken out, blotted the excess water, and weighed immediately. The procedure was repeated until the membrane gained constant weight. The water uptake weight percentage (%) was calculated by the equation:

$$\text{water uptake} \% = [(\text{wet weight} - \text{dry weight})/\text{dry weight}] \times 100$$

The Ag content was determined by inductive coupled plasma emission spectroscopy (ICP-AES) (3300DV, Perkin-Elmer Optima, USA). Briefly, a known amount of CAgNfs was dissolved in HNO_3 and the Ag content was measured by ICP-AES. The surface structure of CAgNfs was examined using FE-SEM (Hitachi S-4800, Japan). Briefly, representative samples of two different CAgNfs (CAgNf-12 and CAgNf-52) were coated with osmium ions using an ion sputter coater under pressure of 0.1 torr and 20 mA current for 70 s (coating time). FE-SEM was operated at an accelerating voltage of 5.0 kV. The atomic-force microscopy (AFM) images of films were obtained using scanning probe microscope (Park system XE-100, Korea). The images of CAgNfs were recorded using digital single lens camera (Canon 1000D, Japan).

In Vitro Antibacterial Activity of CAgNfs

To investigate the antibacterial activity of CAgNfs, three fish pathogenic bacteria species, V. salmonicida (KCTC 2766), V. tapetis (KCTC 12728) and E. tarda (KCTC 12267) were used in this study. Antibacterial activities were investigated by agar disc diffusion assay and modified liquid growth inhibition assay as described previously [16]. CAgNfs were punched to make film discs (8 mm in diameter) and sterilized by autoclaving for 30 min at 120 °C. A single colony from V. salmonicida, V. tapetis and E. tarda was inoculated separately into 4 mL of MB media (Becton, Dickinson, USA), and incubated at 25 °C under shaking (160 rpm) for 16 h. In an agar disc diffusion assay, three bacteria species were inoculated on separate MA plates by spreading overnight culture using sterile cotton tipped swabs under aseptic conditions. Subsequently, sterilized discs of CAgNCs films were immediately impregnated and incubated at 25 °C for 24 h. Antibacterial activity was determined by measuring the diameter of inhibition zone (DIZ) in millimeter scale (including paper disc). Each assay was carried out in triplicates.

For the liquid growth inhibition assay, overnight culture of V. salmonicida, V. tapetis and E. tarda were inoculated into 20 mL of fresh MB media at 1:100 dilution, and then different concentrations (ranging from 25 to 100 µg/mL) of CAgNfs (CAgNf-12 and CAgNf-52) were added to the broth and incubated at 25 °C. Minimum inhibitory concentration (MIC) of CAgNfs was determined according to the method described previously [16]. Different concentrations of CAgNfs were used for MIC determination and the lowest concentration of CAgNfs that inhibits visible growth colonies of bacteria (on MA plate) was considered as MIC. Moreover, the lowest concentration that inhibits the visible growth of the bacteria was considered as minimum bactericidal concentration (MBC).

In Vitro Antifungal Activity of CAgNfs

To investigate the antifungal activity of CAgNfs, a fish pathogenic strain; F. oxysporum isolate CNUaq1 was used. Antifungal activities were investigated by fungal growth restriction assay on PDA plates. Both types of CAgNfs were used for this experiment separately, and the semi-circular pieces of Parafilm® were used as controls in this experiment. Initially, fungal inoculums (3 mm in diameter) were obtained from a growing mycelium edges, and placed at the middle of the PDA plates. Then, growth restriction rings (7.5 mm of internal radius and 15 mm of external radius) were arranged with the initial inoculum using two semi-circular film pieces, one made by para film and the other made by CAgNfs (Fig. 1). All the plates were incubated at 28 °C for 10 days. Fungal cultures were monitored daily to identify the main fungal inhibitory events during the incubation period such as mycelium reaching to inner margin of the restriction ring, mycelium growth over the restriction ring and mycelium spreading over rest of the space. The time taken to grow over the restriction ring by the fungi ($t_{7.5\ mm}$) and the mean radial fungal growth after
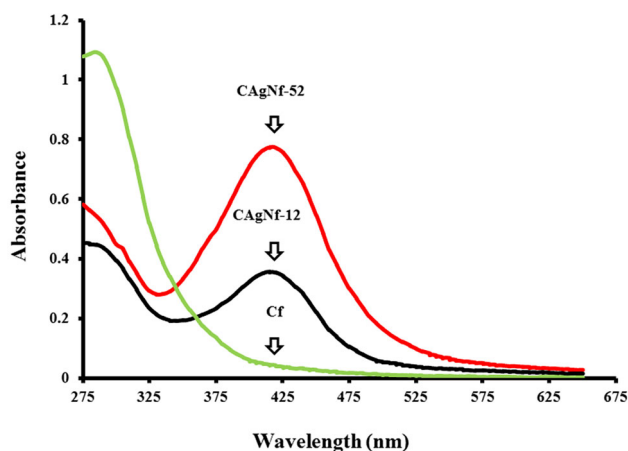
Fig. 1 Ultraviolet visible absorbance patterns of Cf, CAgNf-12 and CAgNf-52

10 days (r_{10d}) were taken as main parameters for assessing antifungal activity (a^o). When fungi grow over the restriction ring, $a^0 \propto t_{7.5\ mm}$ and $a^0 \propto 1/r_{10d}$ the general rule of antifungal activity can be applied.

Reduction of *V. salmonicida* in Seawater by CAgNfs

The bacterial reduction capacity of CAgNfs was determined using viable cell count method on the test pathogenic bacteria *V. salmonicida*. Overnight bacteria culture was inoculated in 20 mL of MB media at 1:100 dilutions. When the bacteria growth reached to the 0.6 of optical density (OD) at 600 nm, cells were harvested by centrifugation (3500 rpm at 4 °C for 10 min), cell pellet was washed, and re-suspended in 10 mL of PBS. Then the bacteria OD was adjusted, and $1x10^6$ cells/mL of *V. salmonicida* was added to 15 mL of artificial seawater (salinity 32%). Then, film samples (100 µg/mL) were cut into the pieces (2.5 × 2.5 cm) and placed in individual flask of *V. salmonicida*. *V. salmonicida* culture without film was maintained as a control. All samples were incubated in an aerobic chamber at 25 °C for 24 h under shaking. Aliquots of 0.1 mL of culture was taken from the flask, diluted serially with 0.1% peptone water, and plated on MA plates to determine the bacteria colony forming units (CFU), which represent the bacteria count in the water. The plates were incubated for 2 days at 25 °C and the number of colonies on each plate were counted, and reported as CFU per milliliter (CFU/mL). Experiment was conducted three times, and average values were used to interpret the data.

Statistical Analysis

Statistical analysis was performed using unpaired, two-tailed *t* test to find the significant differences between the controls and the treatments using GraphPad Prism program

ver. 6 (GraphPad Software, Inc. USA). The significant differences were defined at $P < 0.05$.

Results and Discussion

Preparation and Properties of CAgNfs

In this study, two types of AgNPs impregnated chitosan films were developed using low molecular weight chitosan and AgNO₃. Physiochemical properties (thickness and Ag content) and antimicrobial activities were compared with chitosan film, which was prepared without Ag. Abdelgawad et al. [17] have shown that reaction (reducing) temperature is critical for the reduction of Ag^{+1} into Ag^0 and suggested that 95 °C as the optimum temperature for the formation of AgNPs. Furthermore, chitosan has reducing power, and it can also be used as capping agent which helps to protect from coalescence of AgNPs. For the preparation of CAgNfs, 1% (w/v) low molecular weight chitosan was used as a reducing agent, and maintained at 95 °C. Under this condition, formation of AgNPs in film matrix was observed by the color change from gray to brown with respect to the Cfs. The surface plasmon resonance (SPR) describes the collective excitation of conduction electrons in a metal on interaction with the incident light [18]. In the UV–vis spectra, characteristic SPR absorption band of Ag (at 415 nm) was observed in dispersions of CAgNCs after 3 h of preparation (before casting), which indicates the presence and the level of metallic AgNPs (Fig. 1). A peak at 415 nm was not shown for the Cf, while the highest absorbance at 415 nm was observed for CAgNf-52 solution when compared with the CAgNf-12 solution, suggesting the high shifting could be due to increased level of AgNPs.

The results were further confirmed with the FE-TEM data. The FE-TEM image, particle size distribution and Zeta potential of Cf, CAgNf-12 and CAgNf-52 are shown in Fig. 2. The FE-TEM image of CAgNCs showed no aggregation of AgNPs in chitosan suspension (Fig. 2 a–c). In other words, both CAgNf-12 and CAgNf-52 illustrated a well distribution and high occurrence of AgNPs on Cfs. However, it was found that the CAgNf-52 contains higher particle size AgNPs (12 nm) than CAgNf-12 (9 nm), that could be due to particle agglomeration. The average particle size of Cf (Fig. 2d) obtained from dynamic light scattering (DLS) technique showed relatively higher size distribution (610.4 ± 4.6 nm) than both CAgNf-12 (380.8 ± 10.1 nm) and CAgNf-52 (480.1 ± 6.1 nm) as shown in Fig. 2 e, f, respectively. In CAgNf-52, larger particle size distribution might be a result of AgNPs aggregation. Zeta potential that is surface charge can greatly influences the particle stability in the suspension through the electrostatic repulsion among particles [19].
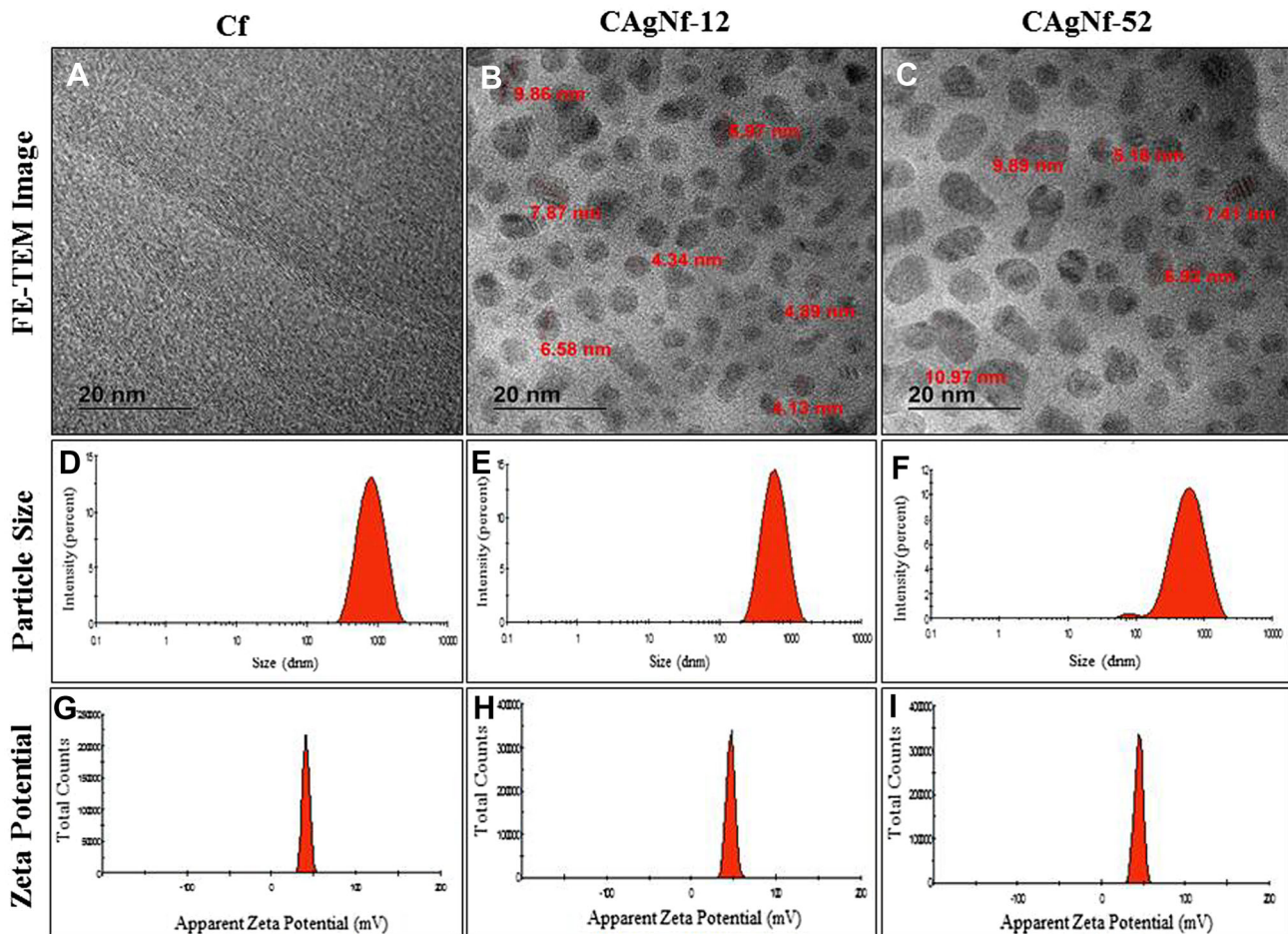
Fig. 2 FE-TEM images, corresponding particle size and zeta potential distributions of chitosan and CAgNCs colloidal solution

Figure 2g shows that the surfaces of Cf suspension have a positive charge of approximately 42.8 ± 3.1 mV, while that of AgNPs loaded CAgNf-12 and CAgNf-52 chitosan suspensions exhibit approximately 44.8 ± 8.6 and 49.2 ± 7.1 mV as shown in Fig. 2h, i, respectively. This positive surface charge might be imparted by protonated amino groups ($-NH_3^+$) of chitosan molecule, which surrounds the particles [20].

Digital and AFM photographs of both CAgNfs (CAgNf-12 and CAgNf-52) were homogenous, flexible and displayed smooth surfaces. However, color variation was correlated with the amount of Ag used for preparation of the films (Fig. 3). Surface color of normal Cf was gray (Fig. 3a), and it showed semitransparent appearance. In contrast, CAgNf-12 and CAgNf-52 displayed light yellowish (Fig. 3b) and brownish tint (Fig. 3c) on surface, respectively. Level of transparency was greatly reduced with the increasing concentration of AgNPs. This could be due to distribution of AgNPs throughout the chitosan polymer matrix. Thin Cfs, CAgNf-12 and CAgNf-52 present different surface topography, when analyzed with AFM (Fig. 3d–f). However, CAgNf exhibits combination of both chitosan and AgNPs surface topography. The CAgNf morphology was dependent upon several factors including polymer solubility, solvent evaporation, total thickness, molecular weight and surface composition [21].

Average thickness of Cf, CAgNf-12 and CAgNf-52 were 35, 25 and 45 μm, respectively (Table 1), and variation of these film thicknesses may be due to compacting differences of chitosan chains during the process of film formation. Moreover, the thicknesses of CAgNfs could be influenced by the concentration of the Ag precursor. The swelling behavior of an antibacterial film is an important aspect of its biomedical applications [4]. Table 1 shows the water uptake behavior of three films in PBS at room temperature. The water uptake of Cf was the highest compared to the CAgNfs. The lowest water uptake was observed for the highest Ag containing film, CAgNf-52 giving evidence that water uptakes of chitosan polymer were restricted with AgNPs. Based on the ICP–AES analysis, it was confirmed that CAgNf-12 and CAgNf-52 contain 4.62 and 16.86% Ag content, respectively. Difference between theoretical and real Ag contents was observed as less than 7% for both CAgNfs. In general, there is a strong correlation between the
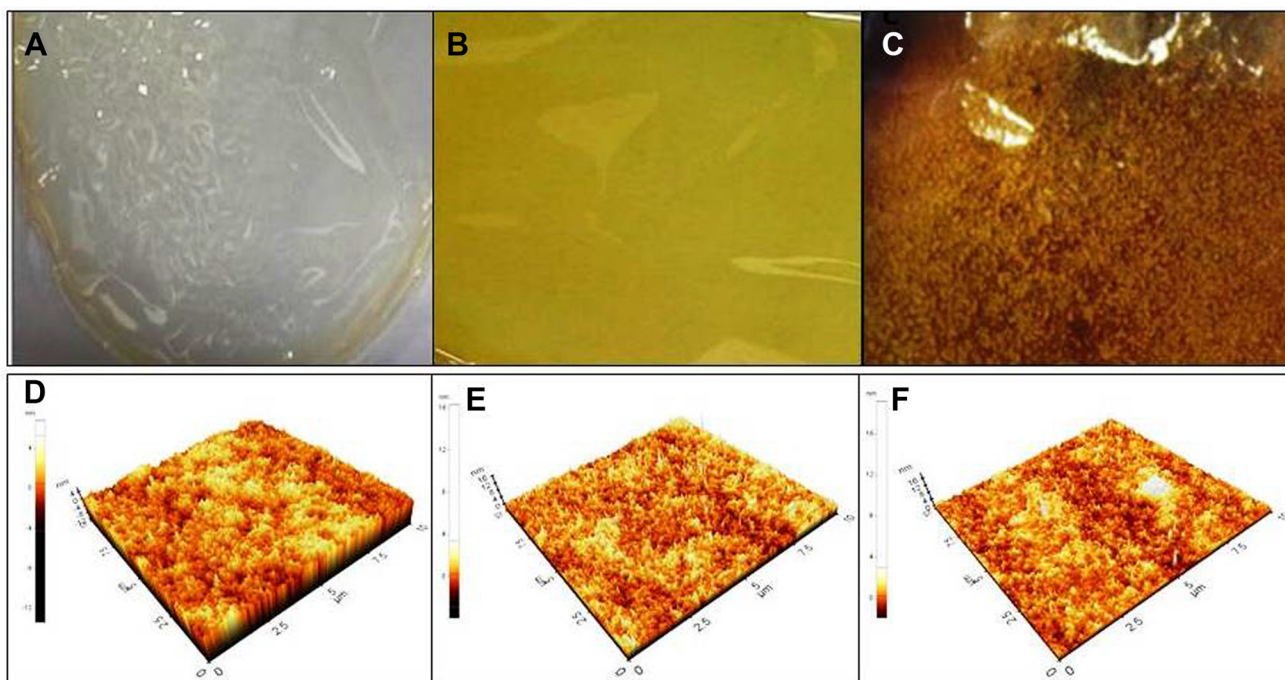
Fig. 3 Digital and AFM photographs of Cf and CAgNfs. Digital: **a** Cf; **b** CAgNf-12 and **c** CAgNf-52. AFM: **d** Cf; **e** CAgNf-12 and **f** CAgNf-52

Table 1 Comparison of thickness, water uptake (%) and AgNPs percentage (%) in Cf and CAgNfs

Type of film	Thickness (μm)	Water uptake (%)	Amount of AgNPs (w/w%) (Theoretical)	Amount of AgNPs (w/w%) (Real-ICP-AES)
Cf	35 ± 5	42.4 ± 5.3	0	0
CAgNf-12	25 ± 10	34.3 ± 2.4	5	4.62 ± 0.28
CAgNf-52	45 ± 10	28.4 ± 1.4	18	16.86 ± 0.36

theoretical values and the results obtained by ICP–AES. As expected, these values tend to be lower than the theoretical Ag content, presumably due to loss of some Ag during film processing at the neutralization and washing steps.

FE-SEM images showed that chitosan polymer helps in nucleation, stabilization and uniform distribution of AgNPs throughout the chitosan matrix (Fig. 4). Moreover, CAgNf-12 and CAgNf-52 showed circular shape AgNPs, which are
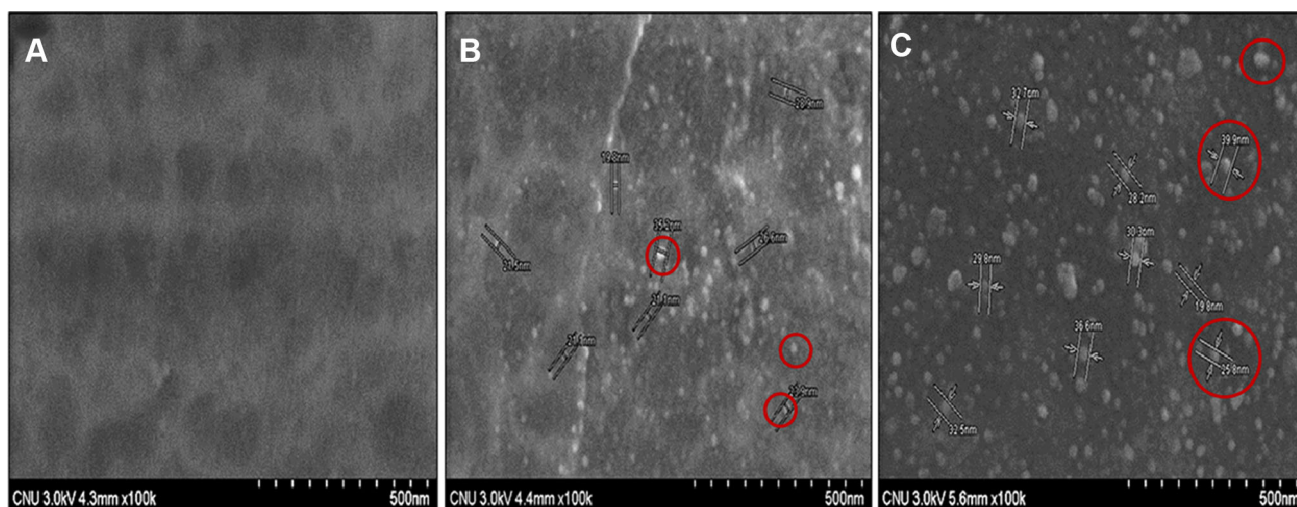

Fig. 4 FE-SEM images of CAgNfs. **a** Cf; **b** CAgNf-12 and **c** CAgNf-52. Circular AgNPs are marked in *red circles* (color figure online)

homogeneously distributed in the films (Fig. 4b, c), whereas the Cf (Fig. 4a) showed complete absence of AgNPs. Additionally, CAgNf-52 exhibited higher particle size of AgNPs (30 nm) than CAgNf-12 (20 nm), suggesting this may be due to particle agglomeration.

In Vitro Antibacterial Activities of CAgNfs

Chitosan has a unique molecular structure, which can deal with microorganisms and toxic materials to clean polluted water. Therefore, we tested the in vitro antibacterial activities of two CAgNfs to find out whether these films can be developed as an antibacterial filters. Antibacterial activities of two CAgNfs were tested against *V. salmonicida*, *V. tapetis* and *E. tarda* as indicator species which are pathogenic to fish. Disc diffusion assay showed that both CAgNfs can inhibit the growth of *V. salmonicida*, *V. tapetis* and *E. tarda* compared to Cf (Fig. 5). However, there was no significant difference ($P < 0.05$) in the growth inhibition of selected three bacteria species between CAgNf-12 and CAgNf-52 that may be due to size variation of AgNPs. The MIC and MBC values for the tested bacteria were given in the Table 2. The MIC of CAgNf-12 and CAgNf-52 against *E. tarda* was 50 and
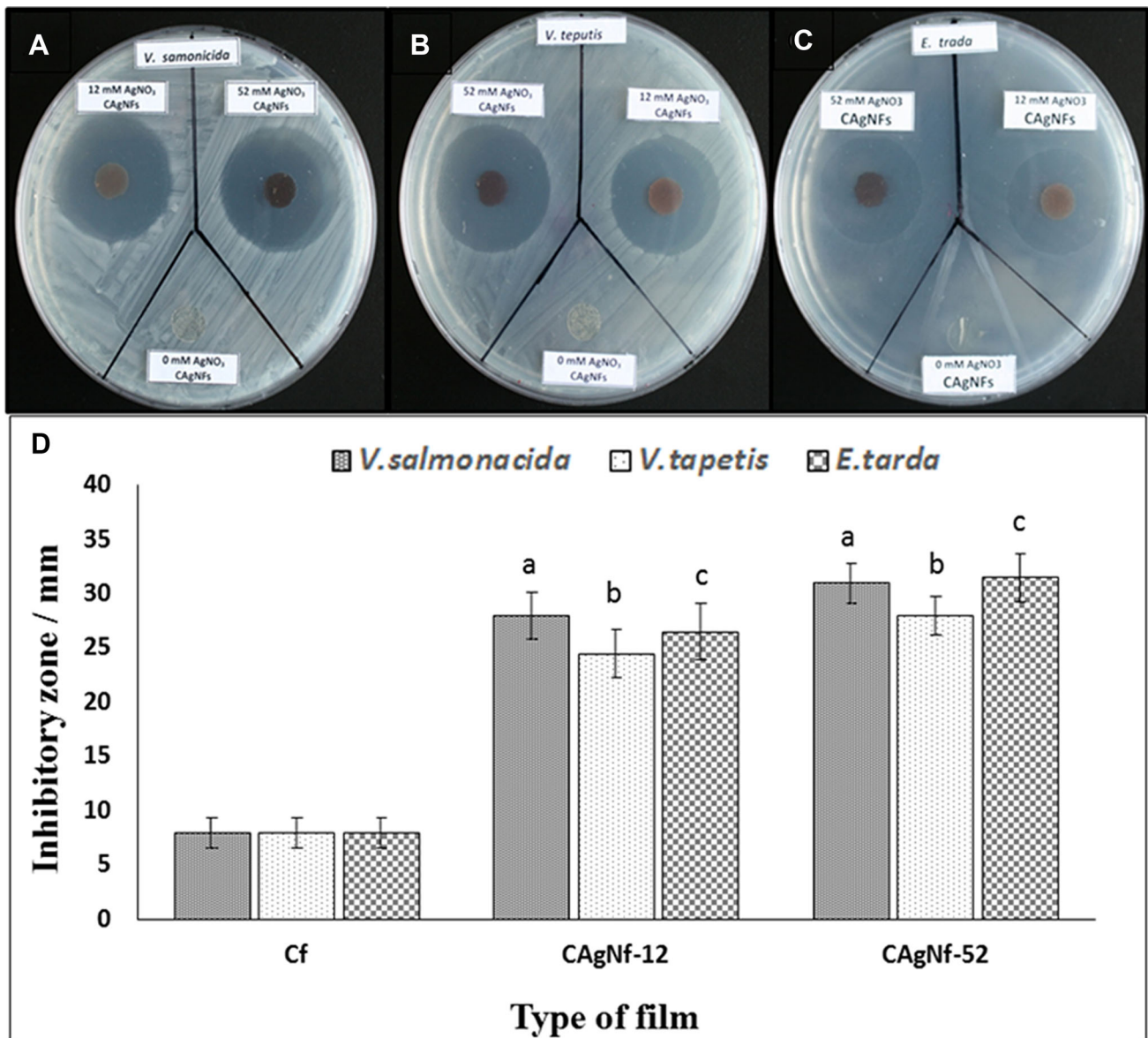

Fig. 5 Images of antibacterial activity assays on marine agar plates **a** *V. salmonicida* **b** *V. tapetis* **c** *E. tarda*, and **d** quantitative disc diffusion assay results. The *error bars* indicate the mean ± S.D. (n = 3). Significant differences ($P < 0.05$) were calculated with respect to controls (Cf), and simple letters (*a*—*V. salmonicida*, *b*—*V. tapetis* and *c*—*E. tarda*) represent the significant differences between control and the CAgNfs corresponding to each bacteria

Table 2 The MIC and MFC values of chitosan and CAgNfs against different bacteria

Type of film	Bacteria name	MIC (µg/mL)	MBC (µg/mL)
CAgNf-12	*V. salmonicida*	75	75
	V. tapetis	75	125
	E. tarda	50	75
CAgNf-52	*V. salmonicida*	50	50
	V. tapetis	75	100
	E. tarda	25	50

25 µg/mL, respectively. Moreover, the highest MIC value, 75 µg/mL was observed for both CAgNf-12 and CAgNf-52 against *V. salmonicida* and *V. tapetis*. The MBC of CAgNf-12 against *V. salmonicida*, *V. tapetis* and *E. tarda* was 75, 125 and 75 µg/mL, respectively. However, for CAgNf-52, the MBC values were changed as 50, 100 and 50 µg/mL for the same species of the bacteria mentioned above.

In Vitro Antifungal Activity of CAgNfs

According to the fungal growth restriction assay results, both types of CAgNfs have effectively inhibited the growth of *F. oxysporum* compared to the control (Fig. 6b). Three days post inoculation, fungal mycelium was spread uniformly within the inner growth circle in all tested plates. Then at 6 days post inoculation, fungal mycelium was overgrown and passed the semicircular parafilm (7.5 mm wide) growth restriction rings (control). However, fungal growth was restricted at semicircular CAgNfs growth

restriction rings indicating irregular and aggregated mycelial growth (at the inner edges) at 6 days post inoculation. Complete mycelial growth was observed at the side of parafilm halves at 10 days post incubation. Total inhibition of fungal growth/fungistatic activity was observed in both types of CAgNfs compared to controls. Antifungal/fungistatic activities of two CAgNfs have been tested with *F. oxysporum*, as it has been reported in fresh water systems [22] and its mycotoxin has been taken as an indicator for water pollutions [23]. Several studies have been reported the lack of measurable zone diameter in disc diffusion assay with several fungi including *Fusarium* [24]. The size of the clear zone in the disc diffusion assay mainly depends on the size of the disc and the inoculum, type of the substrate and the extent of the disc-medium interface [25]. During our experiment, we experienced the same phenomena, and decided that disc diffusion assay for CAgNfs is not efficient with *F. oxysporum* as it grows densely from the center. Fungal growth restriction assay demonstrated in this study was identified as a better measurement to determine the antifungal activity of CAgNfs. Chitosan nano films have potential to inhibit fungi at the contact surface, and it cannot inhibit the fungi remain in the media without direct contact [26]. This gives a clear explanation to the nonexistence of inhibition zone near inner margin of the CAgNfs restriction ring, and the acute mycelial growth decline at the edge of the CAgNfs restriction ring. The productive zone of the fungal mycelium provides the nutrient and other supportive factors to the vegetative leading edge to fly-over the growth restriction ring at the control halves. Due to the inhibitory effect
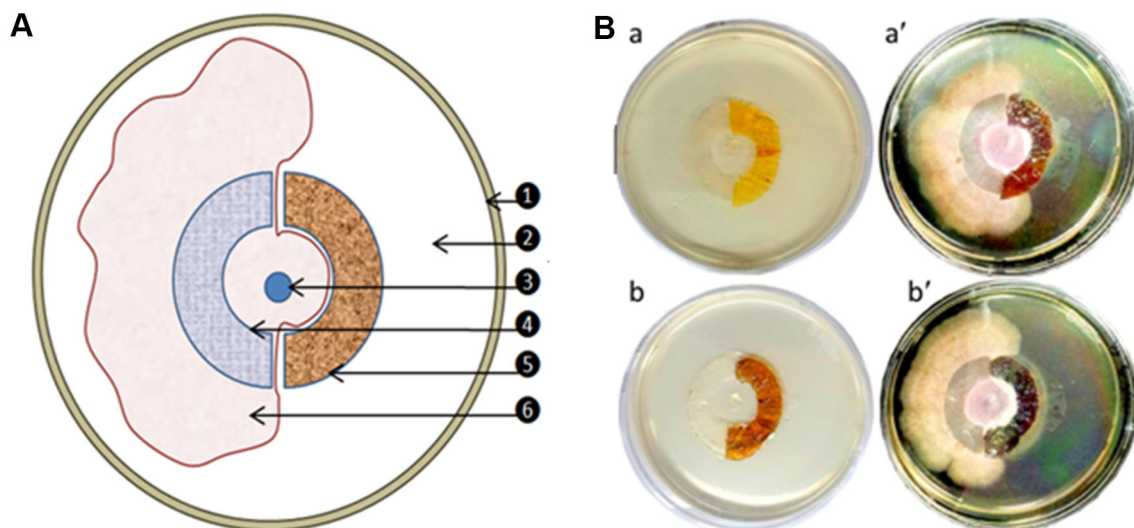

Fig. 6 Schematic diagram of fungal growth restriction assay and antifungal activity of CAgNfs. A: *1* petri dish boundary; *2* PDA media; *3* fungal inoculum (3 mm diameter); *4* semi-circular growth barrier (parafilm/control); *5* semi-circular growth barrier (CAgNfs); *6* fungal growth over the control barrier and spread over the corresponding half of the plate (10 days after inoculation). B: antifungal activity of CAgNf-12 (*a'*) and CAgNf-52 (*b'*) against *F. oxysporum* after 10 days of inoculation. Respective controls are indicated as a and b

on mycelial leading edge, fungi were unable to fly-over the growth restriction ring at CAgNfs halves. These results clearly demonstrate the strong fungistatic/inhibitory properties of CAgNfs.

Control of Bacteria in Seawater by CAgNfs

To prevent diseases, it is important to maintain minimum microbial level, organic compounds, and heavy metals in aquaculture systems. Therefore, we tested two types of CAgNfs (CAgNf-12 and CAgNf-52) to find out, whether they can be practically used in the aquarium model system as a new type of film, with the intention of developing it as antibacterial filters in the future. All the prepared membranes were assessed with *V. salmonicida* as a model bacterium to examine the inhibitory effects. As shown in Fig. 7, after 24 h, *V. salmonicida* count was significantly reduced in both CAgNfs compared to Cf added artificial seawater. Furthermore, inhibition of *V. salmonicida* was slightly higher in CAgNf-52 treated seawater than CAgNf-12. However, after 24 h, *V. salmonicida* level was not completely eliminated in CAgNfs added seawater. Sarasam and Madihally [27] reported that the chitosan based films are not bactericidal, and they only reduced the bacteria growth in liquid culture. Consequently, it can be suggested that complete elimination of bacteria can be reached by increasing the concentration of CAgNfs as well as the exposure time.

Possible Antimicrobial Mechanism of CAgNfs

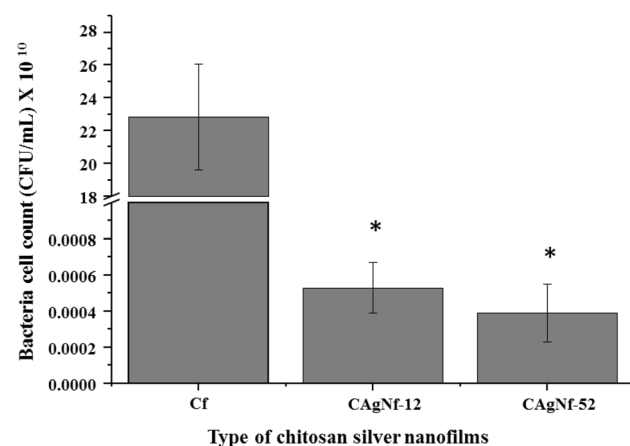Growth inhibition of pathogenic bacteria by nano fibrous membranes combined with Ag as exogenic antibacterial

Fig. 7 Effect of CAgNfs on controlling the *V. salmonicida* in seawater. *V. salmonicida* count in artificial seawater with Cf, CAgNf-12 and CAgNf-52 (100 µg/mL) at 25 °C after 24 h. The bars indicate the mean ± S.D. (n = 3). Significant differences ($P < 0.05$) were calculated with respect to the control (Cf) and marked in *asterisks* (*)

agents such as cellulose acetate/AgNPs, poly vinylidene fluoride/AgNPs and chitosan/polyvinyl alcohol/AgNO₃/TiO₂ have been reported [28–30]. Though the mechanism of chitosan or AgNPs on antibacterial activity has been reported [31], the exact mechanism to explain the antimicrobial activity of CAgNfs is poorly understood yet. Anna et al. [16] reported that, the direct contact between the bacteria and the chitosan–silver films is necessary to achieve a strong antimicrobial action compared with pure chitosan films, and proved that Ag^+ can release from chitosan silver nanocomposite film. Ignatova et al. [32] demonstrated that polycationic chitosan (pure polymeric films) interacts with negatively charged bacterial cell wall and leads to intracellular components leakage, Moreover, Lok et al. [33] concluded that releasing of Ag^+ could not be solely responsible for the strong bactericidal action of AgNPs in chitosan–silver films. In agreement with the previously described probable mechanisms related to antimicrobial activity of AgNPs and the ionic Ag [34, 35], since chitosan film did not show any inhibitory action, we could postulate that growth inhibitory action of CAgNfs in this study also could be due to association of the AgNPs and the ionic Ag with bacteria. It has been reported that AgNPs or Ag ions which is released from the AgNPs could directly affect the cell-membrane morphology [36], interfere with permeability of microbial membrane, cause oxidative stress [37], trigger inactivation of respiratory enzymes, interrupt electron transport [38] and DNA replication [39], and cause even bacteriolysis. However, the exact antimicrobial mechanism of CAgNfs needs to be elucidated in the future.

Conclusions

In conclusions, AgNPs were successfully introduced into chitosan using a green reduction method in order to develop biologically active CAgNfs. Incorporation of Ag was confirmed by the SPR peak at 415 nm for both CAgNfs indicating the formation of AgNPs. Results from disc diffusion and turbidimetric assays clearly indicated that both CAgNfs can inhibit the growth of pathogenic bacteria (*V. salmonicida*, *V. tapetis* and *E. tarda*) as well as fungi *F. oxysporum*. These CAgNfs could be developed or modified into antimicrobial filters/membranes for water filtering units to eliminate the pathogenic bacteria and fungi in future.

Compliance with Ethical Standards

Conflict of interests The authors declare that they have no conflict of interest.

References

1. Bozanic DK, Trandafilovic LV, Luyt AS, Djokovic V (2010) 'Green' synthesis and optical properties of silver–chitosan complexes and nanocomposites. React Funct Polym 70:869–873. doi:10.1016/j.reactfunctpolym.2010.08.001
2. Lu S, Gao W, Gu HY (2008) Construction, application and biosafety of silver nanocrystalline chitosan wound dressing. Burns 34:623–628. doi:10.1016/j.burns.2007.08.020
3. Shen XL, Wu JM, Chen Y, Zha G (2010) Antimicrobial and physical properties of sweet potato starch films incorporated with potassium sorbate or chitosan. Food Hydrocoll. 24:285–290. doi:10.1016/j.foodhyd.2009.10.003
4. Sharma S, Sanpui P, Chattopadhyay A, Ghosh SS (2012) Fabrication of antibacterial silver nanoparticle–sodium alginate–chitosan composite films. RSC Adv 2:5837–5843. doi:10.1039/C2RA00006G
5. Cooper A, Oldinski R, Ma H, Bryers JD, Zhang M (2013) Chitosan-based nanofibrous membranes for antibacterial filter applications. Carbohydr Polym 92:254–259. doi:10.1016/j.carbpol.2012.08.114
6. Velmurugan P, Lydroose M, Lee SM, Cho M, Park JH, Balachandar V, Oh BT (2014) Synthesis of silver and gold nanoparticles using cashew nut shell liquid and its antibacterial activity against fish pathogens. Indian J Microbiol 54(2):196–202. doi:10.1007/s12088-013-0437-5
7. Bose D, Chatterjee S (2015) antibacterial activity of green synthesized silver nanoparticles using Vasaka (Justicia adhatoda L.) leaf extract, Indian. J Microbiol 55(2):163–167. doi:10.1007/s12088-015-0512-1
8. Bozanic DK, Brankovi SD, Bibic N, Luyt AS, Djokovic V (2011) Silver nanoparticles encapsulated in glycogen biopolymer: morphology, optical and antimicrobial properties. Carbohydr Polym 83:883–890. doi:10.1016/j.carbpol.2010.08.070
9. Huang H, Yang X (2004) Synthesis of chitosan-stabilized gold nanoparticles in the absence/presence of tripolyphosphate. Biomacromol 5:2340–2346. doi:10.1021/bm0497116
10. Guo Y, Yan H (2008) Preparation and characterization of heparin-stabilized gold nanoparticles. J Carbohydr Chem 27:309–319. doi:10.1080/07328300802158752
11. Vigneshwaran N, Nachane RP, Balasubramanya RH, Varadarajan PV (2006) A novel one-pot 'green' synthesis of stable silver nanoparticles using soluble starch. Carbohydr Res 341:2012–2018. doi:10.1016/j.carres.2006.04.042
12. Anastas PT, Williamson TC (1998) Frontiers in green chemistry. In: Anastas PT, Williamson TC (eds) Green chemistry: frontiers in benign chemical syntheses and processes. Oxford University Press, USA
13. Liu S, He J, Xue J, Ding W (2009) Efficient fabrication of transparent antimicrobial poly (vinyl alcohol) thin films. J Nanopart Res 11:553–560. doi:10.1007/s11051-007-9321-8
14. Arockianathan PM, Sekara S, Kumaran B, Sastrya TP (2012) Preparation, characterization and evaluation of biocomposite films containing chitosan and sago starch impregnated with silver nanoparticles. Int J Biol Macromol 50:939–946. doi:10.1016/j.ijbiomac.2012.02.022
15. Rujitanaroj PO, Pimpha N, Supaphol P (2008) Wound-dressing materials with antibacterial activity from electrospun gelatin fiber mats containing silver nanoparticles. Polymer 49:4723–4732. doi:10.1016/j.polymer.2008.08.021
16. Regiel A, Irusta S, Kyzioł A, Arruebo M, Santamaria J (2013) Preparation and characterization of chitosan–silver nanocomposite films and their antibacterial activity against Staphylococcus aureus. Nanotechnology 24:015101. doi:10.1088/0957-4484/24/1/015101
17. Abdelgawad AM, Hudson SM, Rojas OJ (2014) Antimicrobial wound dressing nanofiber mats from multicomponent (chitosan/silver-NPs/polyvinyl alcohol) systems. Carbohydr Polym 100:166–178. doi:10.1016/j.carbpol.2012.12.043
18. Sonawane S, Jacob B, Mallick R, Mohanty S, Jena P (2012) Toxicity and antibacterial assessment of chitosan coated silver nanoparticles on human pathogens and macrophage cells. Int J Nanomed 7:1805–1818. doi:10.2147/IJN.S28077
19. Du WL, Niu SS, Xu XL, Xu ZR, Fan CL (2009) Antibacterial activity of chitosan tripolyphosphate nanoparticles loaded with various metal ions. Carbohydr Polym 75:385–389. doi:10.1016/j.carbpol.2008.07.039
20. Yoksan R, Chirachanchai S (2010) Silver nanoparticle-loaded chitosan–starch based films: fabrication and evaluation of tensile, barrier and antimicrobial properties. Mater Sci Eng C 30:891–897. doi:10.1016/j.msec.2010.04.004
21. Ahmad MB, Lim JJ, Shaameli K, Ibrahim NA, Tay MY (2011) Synthesis of silver nanoparticles in chitosan, gelatin and chitosan/gelatin bio nanocomposites by a chemical reducing agent and their characterization. Molecules 16:7237–7248. doi:10.3390/molecules16097237
22. Sautour M, Edel-Hermann V, Steinberg C, Sixt N, Laurent J, Dalle F et al (2012) Fusarium species recovered from the water distribution system of a French university hospital. Int J Hyg Environ Health 215:286–292. doi:10.1016/j.ijheh.2011.11.003
23. Gromadzka K, Waskiewicz A, Swietlik J, Bocianowski J, Golinski P (2015) The role of wastewater treatment in reducing pollution of surface waters with zearalenone. Arch Ind Hyg Toxicol 66:159–164. doi:10.1515/aiht-2015-66-2606
24. Maida CM, Milici ME, Trovato L, Oliveri S, Amodio E, Spreghini E, Scalise G, Barchiesi F (2008) Evaluation of the disk diffusion method compared to the microdilution method in susceptibility testing of anidulafungin against filamentous fungi. J Clin Microbiol 46:4071–4074. doi:10.1128/JCM.01088-08
25. Rhim JW, Hong SI, Park HM, Ng PKW (2006) Preparation and characterization of chitosan-based nanocomposite films with antimicrobial activity. J Agric Food Chem 54:5814–5822. doi:10.1021/jf060658h
26. Mihai AL, Tanase EE, Popa ME (2015) Comparative in vitro study of the chitosan application method effect on Aspergillus brasiliensis growth. Romanian Biotechnol Lett 20:10751–10757
27. Sarasam A, Madihally S (2005) Characterization of chitosan–polycaprolactone blends for tissue engineering applications. Biomaterials 26:5500–5508. doi:10.1016/j.biomaterials.2005.01.071
28. Ramaseshan R, Sundararajan S, Jose R (2007) Nanostructured ceramics by electrospinning. J Appl Phys 102:111101. doi:10.1063/1.2815499
29. Son B, Yeom BY, Song SH, Lee CS, Hwang TS (2009) Antibacterial electrospun chitosan/poly(vinyl alcohol) nanofibers containing silver nitrate and titanium dioxide. J Appl Polym Sci 111:2892–2899. doi:10.1002/app.29233
30. Yuan J, Gang J, Xing Z, Shen J, Kang IK, Byun H (2010) Electrospinning of antibacterial poly (vinylidene fluoride) nanofibers containing silver nanoparticles. J Appl Pol Sci 116:668–672. doi:10.1002/app.31632
31. Prema P, Thangaoandiyan S (2013) In-Vitro antibacterial activity of gold nanoparticles capped with polysaccharide stabilizing agents. Int J Pharm Pharm Sci 5:310–314

32. Ignatov M, Manolova N, Rashkov I (2007) Novel antibacterial fibers of quaternized chitosan and poly (vinyl pyrrolidone) prepared by electro spinning. Eur Polym J 43:1112–1122. doi:10.1016/j.eurpolymj.2007.01.012

33. Lok CN, Ho CM, Chen R, He QY, Yu WY, Sun H et al (2007) Silver nanoparticles: partial oxidation and antibacterial activities. J Biol Inorg Chem 12:527–534. doi:10.1007/s00775-007-0208-z

34. Duran N, Marcato PD, De Conti R, Alves OL, Costa FTM, Brocchi M (2010) Potential use of silver nanoparticles on pathogenic bacteria, their toxicity and possible mechanisms of action. J Braz Chem Soc 21:949–959. doi:10.1590/S0103-50532010000600002

35. Dakal TC, Kumar A, Majumdar RS, Yadav V (2016) Mechanistic basis of antimicrobial actions of silver nanoparticles Front Microbiol 7:1831. doi:10.3389/fmicb.2016.01831

36. Hsueh YH, Lin KS, Ke WJ, Hsieh CT, Chiang CL, Tzou DY, Liu ST (2015) The Antimicrobial properties of silver nanoparticles in *Bacillus subtilis* are mediated by released Ag$^+$ ions. PLoS ONE 10:e0144306. doi:10.1371/journal.pone.0144306

37. Belluco S, Losasso C, Patuzzi I, Rigo L, Conficoni D, Gallocchio F, Cibin V, Catellani P, Segato S, Ricci A (2016) Silver as antibacterial toward *Listeria monocytogenes*. Front Microbiol 7:307. doi:10.3389/fmicb.2016.00307

38. Matsumura Y, Yoshikata K, Kunisaki S, Tsuchido T (2003) Mode of bactericidal action of silver zeolite and its comparison with that of silver nitrate. Appl Environ Microbiol 69:4278–4281. doi:10.1128/AEM.69.7.4278-4281.2003

39. Feng QL, Wu J, Chen GQ, Cui FZ, Kim TN, Kim JO (2000) A mechanistic study of the antibacterial effect of silver ions on *Escherichia coli* and *Staphylococcus aureus*. J Biomed Mater Res 52:662–668. doi:10.1002/1097-4636(20001215)52:4<662:AID-JBM10>3.0.CO;2-3